ACS Biomaterials SCIENCE & ENGINEERING

pubs.acs.org/journal/abseba

Review

Combining Radiotherapy (RT) and Photodynamic Therapy (PDT): Clinical Studies on Conventional RT-PDT Approaches and Novel Nanoparticle-Based RT-PDT Approaches under Preclinical Evaluation

Dhushyanth Viswanath and You-Yeon Won*

Cite This: https://doi.org/10.1021/acsbiomaterials.2c00287

Read Online

ACCESS | Metrics & More | Article Recommendations

ABSTRACT: Radiotherapy (RT) is the primary standard of care for many locally advanced cancers. Often times, however, the efficacy of RT is limited due to radioresistance that cancer cells develop. Photodynamic therapy (PDT) has gained importance as an alternative local therapy. Because its mechanism involves minimal acquired resistance, PDT is a useful adjunct to RT. This review discusses recent advances in combining RT with PDT for cancer treatment. In the first part of this review, we will discuss clinical trials on RT + PDT combination therapies. All these approaches suffer from the same inherent limitations as any current PDT methods; (i) visible light has a short penetration depth in human tissue (<∼10 mm), and (ii) it is difficult to illuminate the entire tumor homogeneously by external/interstitial laser irradiation. To address these limitations, scintillating nanoparticle-mediated RT-PDT approaches have been explored in which nanoparticles convert X-rays (RT) into visible light (PDT); high-energy X-rays can reach deep into the body to irradiate cancers uniformly and precisely. The second part of this review will discuss recent efforts in developing and applying nanoparticles for RT-PDT applications.

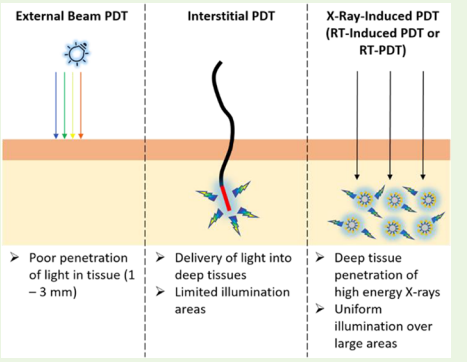

KEYWORDS: *radiotherapy, photodynamic therapy, scintillating nanoparticle, radioluminescent nanoparticle, semiconductor nanoparticle, photosensitizer, Cherenkov radiation*

1. INTRODUCTION

The last two decades have seen a steady decline in annual cancer incidence and mortality rates.[1] While progress in diagnosis and treatment has been made with regards to various types of cancers, this trend has largely been attributed to a decline in incidence and improved management of the four major cancer types (lung, breast, prostate, and colorectal).[1] Despite improvements in standard therapies including surgery, radiotherapy, and chemotherapy, many cancers still carry a poor prognosis even when detected at an early stage.[2−5]

During the period since the discovery of X-rays by Röntgen in 1895, radiotherapy (RT) has been extensively used for cancer treatment.[6] Irradiation technology has significantly evolved from using heated-cathode X-ray tubes to linear accelerators that are capable of producing X-rays of megavolt energy.[6] This development has enabled the use of RT for treatment of deep-seated tumors. Currently, RT is the primary treatment modality for about 29% of all cancer survivors in the US, with intensity-modulated radiotherapy (IMRT), stereotactic radiosurgery, or image-guided RT being the standard of RT in the clinic.[7,8] While these state-of-the-art procedures enabled significant improvements in dose localization, the effectiveness of RT is still limited because of the inherent incompatibility of the treatment with the nature of the cancer,[9,10] or the difficulty of implementing the treatment to a desired effect while controlling side effects.[11,12] For this reason, researchers have been seeking to develop an improved treatment modality that involves a new (more effective and safer) biological mechanism, for use as a standalone treatment or in combination with a conventional therapy.

2. PHOTODYNAMIC THERAPY

One such therapy that has received growing attention over the past few decades because of its noninvasive/highly localized nature is photodynamic therapy (PDT).[13] PDT produces therapeutic effects as a result of interactions among three individually benign components: namely, visible light photons,

Received: March 9, 2022
Accepted: August 12, 2022

molecular oxygen (O_2), and a photosensitizing agent (photosensitizer or PS). Upon photoexcitation, photosensitizers are converted from a ground to excited singlet state prior to undergoing intersystem crossing to a lower-energy, longer-lived triplet excited state. From either excited state, photosensitizers react with biological substrates to form unstable radical species which subsequently undergo reactions with molecular oxygen to generate cytotoxic reactive oxygen species (ROS), such as hydroxide radicals ($^{\bullet}OH$), hydrogen peroxide (H_2O_2), and superoxide anions ($O_2^{\bullet-}$). This process of forming ROS via intermediate radicals is called the type I photodynamic reaction. More common is the type II photodynamic reaction, in which a triplet excited PS directly transfers energy to molecular oxygen (in the triplet ground state), which then turns into singlet oxygen ($^1O_2$). $^1O_2$ and other ROS are very short-lived, with half-lives ranging from about 0.03 to 0.18 ms in biological media, and therefore their effects are confined within short distances near their sites of production.[14] As a result, the primary mode of photodynamic cytotoxicity is largely controlled by the location of photosensitizers; for instance, hydrophobic photosensitizers are localized within the interior of lipid membranes and thus cause cell death by compromising the integrity of cell/organelle membranes. This is a simplistic overview of the PDT mechanism. Detailed discussions are available in the literature.[15−17]

2.1. Progress in Clinical Applications of Photodynamic Therapy. The initial testing of PDT in the early 1900s was motivated by the observation of the phototoxicity of hematoporphyrin in human skin.[18] Following the discovery of selective accumulation of porphyrins in tumors[19] and innovations in PS design,[20] PDT's potential in oncology was first demonstrated when a complete tumor response to hematoporphyrin and red light was observed by Dougherty et al. in mice bearing mammary tumors.[21] Subsequent work by the same group verified high rates of response to PDT in human patients with various tumors, both cutaneous and subcutaneous.[22] These and other studies demonstrated the usefulness of PDT for treatment of cutaneous lesions. However, higher PS doses and longer exposure to external light were required to produce therapeutic effects in subcutaneous lesions, because visible light has a very limited penetration depth in human/animal tissue (<10 mm).[22] Also, off-target irradiation causes side effects.[17] To address these limitations of external-beam PDT, interstitial PDT, in which laser light is delivered through an optical fiber inserted via a needle or catheter directly into the tumor or the tissue around it, has been developed. Although it offers advantages in light delivery, interstitial PDT suffers from nonuniform exposure of the tumor to the light, which results in incoherent responses within the tumor.[23] Shafirstein et al.[23] have reviewed recent clinical trials of interstitial PDT in patients with various cancer types. PDT is now an established modality of cancer treatment with several FDA-approved photosensitizers (7 approved plus 7 under clinical investigation as of 2018),[24] including aminolevulinic acid and methyl aminolevulinate for topical application and porfimer sodium and temoporfin for systemic administration.[16]

3. COMBINATION OF RADIOTHERAPY AND PHOTODYNAMIC THERAPY

Aside from being used as a standalone treatment, PDT has also been used in combination with a conventional therapy, particularly, in combination with RT, either concurrently or as an adjuvant (adjunct) to conventional RT. This RT-PDT combination is an attractive approach because RT and PDT cause cancer cell death by different mechanisms (although both treatment methods involve the formation of cytotoxic ROS). RT typically inflicts cellular damage at the DNA level (primarily DNA double-strand breakage), which leads to cell death, predominantly by apoptosis and mitotic failure and also, to a lesser extent, by senescence and autophagy.[25] However, certain genetic mutations render cancer cells incapable of initiating apoptosis in response to irreparable DNA damage, and as a result, the cancer cells become resistant to RT.[26] To the contrary, in the PDT case, damage is localized at the subcellular sites of PS accumulation. Conventional photosensitizers typically accumulate in the cell and mitochondrial membranes, and therefore, PDT causes cellular damage in those locations,[14,27,28] which results in cell death via necrosis (in the case of cell membrane damage) or cytochrome-*c*-initiated apoptosis (in the case of mitochondrial membrane damage).[29,30] Due to its unique mechanisms of action, PDT is a powerful complement to RT.

3.1. Photodynamic Therapy as a Salvage Treatment Following Radiotherapy. PDT has been commonly used as a salvage procedure for patients with recurrent cancer post-RT; this practice has shown promising results. For instance, Tan and co-workers used temoporfin (Foscan, 5,10,15,20-tetra(*m*-hydroxyphenyl)chlorin) to treat patients with end-stage head and neck squamous cell carcinoma.[31] All 39 patients (mean age 60.9 years) presented tumors ≤10 mm in depth. 100, 95, and 33% of the patients had undergone prior surgery, RT, and chemotherapy, respectively. After the exhaustion of conventional treatment options, the patients received PDT involving an intravenous (IV) administration of 0.15 mg/kg temoporfin followed by illumination of the lesion using a microlens fiber connected to a diode laser (λ_{max} = 652 nm) within 96 h of temoporfin administration; extreme caution was taken to illuminate the entire tumor. The results were promising; the overall response rate was 68%, and the median progression-free survival times were 33 months in patients with tumors showing responses and 2.5 months in patients with nonresponding tumors. The overall median survival times were 37 months for responders and 7.4 months for nonresponders; 8 responding patients survived as of the latest follow-up. Side effects were mild to moderate with short-term photosensitivity at the site of treatment being the most common one.

In another study[32,14] patients (median age 70 years) with unresectable recurrent adenocarcinoma in the prostate gland (as determined by an increase in prostate-specific antigen (PSA)) underwent PDT with temoporfin (IV administered at a dose of 0.15 mg/kg). All the patients received prior external beam RT (40−64 Gy). Tumors were irradiated at 3 days post-RT using a diode laser (λ_{max} = 652 nm) with a laser fiber inserted through a needle inserted percutaneously into the prostate gland. Treatment response was measured by X-ray CT/contrast enhanced MRI and by PSA levels. Image analysis showed significant tissue necrosis in most treated tumors (up to 91% of the prostate cross section); five patients had no visible tumor remaining. Nine patients demonstrated a decrease in PSA level by up to 79%; two of them had a full remission of the disease. Furthermore, PDT was generally well tolerated with side effects including further exacerbation of the loss of erectile function (already significantly impaired due to the initial RT) and acute discomfort during urination. The

https://doi.org/10.1021/acsbiomaterials.2c00287
ACS Biomater. Sci. Eng. XXXX, XXX, XXX−XXX

authors mentioned that light delivery was done conservatively because interstitial illumination was unprecedented at that time; some regions of the prostate were left unirradiated. They speculated that the complete illumination of the prostate using an accurate dosimetry system may allow ablation of the entire lesion.

Yet, in another study,[33] PDT was given after external beam RT to 24 patients (mean age unreported) with recurrent prostate carcinoma. Palladium-bacteriopheophorbide (Tookad), which targets tumor vasculature and impairs blood supply to the tumor, was used as the PS. The study was designed to evaluate the safety of palladium-bacteriopheophorbide with two treatment arms: one in which patients received a fixed light dose (100 J/cm) but escalating drug doses (0.1−2.0 mg/kg), and the other with a fixed drug dose (2 mg/kg) but escalating light doses (100−360 J/cm). A bundle of optical fibers, each inserted through a closed-end catheter, encased within a modified brachytherapy frame and connected to a diode laser (λ_{max} = 763 nm) was inserted transperineally into the prostate. Palladium-bacteriopheophorbide was administered intravenously, and then 20 min were allowed to pass before RT was started. Treatment response was assessed by PSA levels and MRI scans. Results suggested a positive correlation between drug/light dosage and their effect. The largest bilateral lesions were found in 6 patients treated with the highest drug/light doses; in this group, the average lesion diameter was 22 ± 6 mm, which corresponded to >20% of the total prostate volume. The PSA levels in 4 out of the 6 patients had reduced to a negligible level and remained at that level until the last follow-up 6 months later. No serious mid- to long-term adverse effects were noted such as prolonged photosensitivity (often observed with other photosensitizers). This is due to the very short half-life of palladium-bacteriopheophorbide in the body (∼20 min). There was some variation in treatment response at an identical light dose, which was attributed to inconsistency in light illumination.

PDT has also been used for the treatment of malignant brain tumors. In a study conducted by Muller and Wilson,[34] 50 patients (mean age 48 years) with malignant supratentorial tumors were chosen; out of the 50 patients, 45 had cerebral glioma, whereas the other 5 had solitary cerebral metastasis. 33 out of the 50 patients had recurrent disease after previous treatment (surgery/RT). Tumors were treated with a PS, a hematoporphyrin derivative (Photofrin I) or dihematoporphyrin ether (Photofrin II), administered intravenously at a dose of 2 or 5 mg/kg. At 18−24 h post-PS injection, tumors were irradiated intraoperatively using a custom-built illuminator composed of an inflatable balloon applicator coupled to an argon dye pump laser (λ_{max} = 630 nm). Immediately prior to illumination, tumors were debulked by resection or draining fluid from the cyst. Twelve patients whose tumor geometries allowed complete illumination of the tumor demonstrated complete or near-complete responses. The median survival time of this group was 17.1 months, which was significantly greater than that of the remaining cases (6.5 months). A significant survival benefit was also noted for higher doses of light (>1500 J) relative to lower doses. The treatment was generally well tolerated except for some instances of cerebral edema in cases involving illumination over large areas. The authors concluded that treatment success was critically dependent on light delivery; better prognosis was achieved with a more complete/homogeneous distribution of light across the tumor.

3.2. Photodynamic Therapy as a Neoadjuvant Treatment to Radiotherapy. Aside from its use as a salvage treatment, PDT has also often been used as a neoadjuvant to RT. Umegaki and colleagues have used PDT to debulk cutaneous anaplastic large cell lymphoma prior to RT.[35] In this single patient study, 5-aminolevulinic acid (ALA) (20% in Dortin) was topically applied, and the tumor was externally irradiated with a halide lamp (λ_{max} = 630−700 nm) at 6 h post-ALA administration. The tumor was nearly completely debulked and thus became suitable for external beam RT (40 Gy total). The patient experienced no significant side effects aside from some tolerable pain in the illuminated area and remained disease free up to the last follow-up visit at 2 years post-treatment. Results from *in situ* TUNEL assay showed that, following PDT, cancer cell death occurred predominantly via necrosis rather than apoptosis, which makes this PDT → RT treatment more beneficial than RT alone or chemotherapy alone for localized lesions.

Lam and co-workers used PDT in combination with palliative external beam RT to treat patients with inoperable obstructive non-small cell bronchogenic carcinoma for comparison with palliative RT alone.[36] A total of 11 patients (mean age 66 years) were randomized into either group. Patients in the dual treatment arm underwent PDT first. Photofrin II was injected intravenously 24−48 h prior to light illumination. An Ar-pumped dye laser (λ_{max} = 630 nm) was inserted into a fiberoptic bronchoscope for tumor illumination. All patients received a total of 30 Gy X-ray dose delivered over 2 weeks. The results indicated a significant difference between the two groups; all patients treated with RT only showed tumor regrowth after 12 weeks of treatment, and three of them died before the subsequent follow-ups at 22, 36, and 37 weeks, whereas only 1/4 of the patients who received the dual treatment showed relapse of the disease during the 12-week period, and 2 patients were in complete remission at 26 and 44 weeks. Benefits of the dual treatment were also noted in terms of respiratory symptoms, breathing status, pulmonary function, and gas exchange. No significant adverse reactions were observed in either group except for mild dysphagia, photosensitivity of the treated areas, and nausea. The authors suggested that the PDT + RT combination would be useful not only for palliative care but also as a primary treatment option.

Further examples of application of PDT + RT in lung cancer treatment include the study of Imamura and co-workers,[37] wherein 29 patients (mean age 67.3 years) with occult lung cancer were treated with either PDT alone or PDT followed by thoracic RT (60 Gy). PDT was performed with the photosensitizer, Photofrin II, administered intravenously (2 mg/kg). Light illumination was performed 48 h later using an argon dye laser/excimer dye laser system (λ_{max} unspecified) attached to a quartz fiber passed through a fiberoptic bronchoscope. One month follow-ups indicated that initial PDT showed a 64% complete response rate, whereas the remainder of the cases showed a complete response rate of 71.4% after subsequent thoracic RT. Overall, 9 patients showed recurrence during the follow-up period which ranged from 4.4 to 75.5 months. Side effects included varying levels of erythema, blister formation on sunlight-exposed skin, and mild airway stenosis; all these side effects were deemed tolerable.

Calzavara and co-workers used PDT or PDT followed by RT to treat superficial esophageal cancer.[38] In this study, 21 patients (median age 61 years) underwent PDT with a hematoporphyrin derivative and hematoporphyrin adminis-

https://doi.org/10.1021/acsbiomaterials.2c00287
ACS Biomater. Sci. Eng. XXXX, XXX, XXX−XXX

Table 1. Summary of the Parameters and Results of the PDT + RT Clinical Studies Discussed in This Review

Cancer Type	Number of Patients	Photosensitizer	PS Administration Route and Dose	Illumination Source	Illumination Parameters	Overall Response Rate of RT + PDT	Main Side Effects	Ref
Recurrent head and neck squamous cell carcinoma	39	Meso-tetrahydroxyphenyl chlorin (Foscan)	IV, 0.15 mg/kg body wt.	Diode laser (652 nm)	Dose = 20 J/cm^2, intensity = 100 mW/cm^2	68%[a]	Mild photosensitivity, pain at the treatment site	31
Recurrent prostate adenocarcinoma	14	Meso-tetrahydroxyphenyl chlorin (Foscan)	IV, 0.15 mg/kg body wt.	Diode laser (652 nm)	100−150 mW, fiber delivered through a urinary catheter	Not characterized[a]	Prolonged loss of erectile function	32
Recurrent prostate carcinoma	24	Tookad	IV, 0.1−2 mg/kg body wt.	Diode laser (763 nm)	100−360 J/cm, delivered through a urinary catheter	Not characterized[a]	Acute impairment of urinary function, intraoperative hypotension	33
Cerebral glioma/solitary cerebral metastasis	50	Photofrin I/Photofrin II	IV, 2−5 mg/kg body wt.	Argon dye pump laser (630 nm)	8−175 J/cm^2	35%[a]	Cerebral edema	34
Cutaneous lymphoma	1	ALA	Topical (20% in Dortin)	Halide lamp (630 − 700 nm)	120 J/cm^2	Not applicable	Tolerable pain at the tumor site during illumination	35
Obstructive non-small cell bronchogenic carcinoma	11	Photofrin II	IV, Dose unspecified	Argon dye pump laser (630 nm)	300 J/cm, delivered through a cylindrical diffuser tip inserted into tumor	Not characterized	Mild dysphagia, photosensitivity of the treated area	36
Roentgenologically occult lung cancer	39	Photofrin II	IV, 2 mg/kg body wt.	Argon dye pump laser (488−514.5 nm and 590−640 nm) or excimer dye laser (λ unspecified)	100−600 J/cm^2, delivered through a fiberoptic bronchoscope	90%	Skin photosensitivity, airway stenosis	37
Esophageal carcinoma	21	Hematoporphyrin and hematoporphyrin derivative	IV, 2.5−5 mg/kg body wt.	Argon dye pump laser	60−205 J/cm^2	52%	Skin photosensitivity	38
Obstructive endobronchial NSCLC	9	Photofrin	IV, 2 mg/kg body wt.	Diode laser (630 nm)	200 J/cm^2, delivered through a bronchoscope with a diffuser attachment	Not characterized	Soft tissue contraction	39
Bowen's disease	4	ALA	Topical (20% in an aqueous cream)	Excimer pumped dye laser (630 nm)	50 J/cm^2 × 4	100%	None	40

[a]Studies in which PDT was used as a salvage treatment following RT.

https://doi.org/10.1021/acsbiomaterials.2c00287
ACS Biomater. Sci. Eng. XXXX, XXX, XXX−XXX

tered intravenously at 2.5 and 5 mg/kg, respectively. Illumination was performed at 24−48 h post-PS injection using an argon dye laser system with a microlens tip. 38% of the patients showed complete response, whereas 28% showed partial response. Within this responsive subgroup, patients who additionally received subsequent RT showed no recurrence for 7−34 months post-treatment. Interestingly, the authors observed a negative correlation between light dose and complete response rate, which was contradictory to what was known in the literature. They attributed this discrepancy to the instability of the light diffusing material in the laser system at high irradiances, fluctuations in emission wavelength, and/or inconsistent delivery of the photosensitizer. Nevertheless, the results supported that PDT → RT is more beneficial than PDT alone.

3.3. Systematic Investigation of Combined Radiotherapy and Photodynamic Therapy. Recently, systematic studies have been conducted to evaluate the synergism between RT and PDT. Weinberg and colleagues designed a study to observe the effect of the order of treatments on tumor control.[39] Nine patients (median age 63 years) with obstructive endobronchial non-small cell lung cancer (NSCLC) were given combined PDT (with 2 mg/kg Photofrin) and high dose rate brachytherapy (15 Gy total). Illumination was done at 24 h after intravenous injection of Photofrin using a diode laser (λ_{max} = 630 nm) fitted with an optical fiber inserted through a bronchoscope. The results favored the use of brachytherapy prior to PDT, which showed local control in 6/7 patients for prolonged periods (3 months to 5+ years); one failed case was due to systemic spread of the disease. When PDT preceded RT, 2/2 patients showed partial response; local palliation was achieved in one patient only for 10 weeks. It was observed that the shorter the interval between the treatments, the more prolonged the tumor control, and that the combination of the two treatments was generally well tolerated. The authors noted that uneven light dose distribution might have affected the efficacy of PDT. The overall conclusion of the study was that brachytherapy followed by PDT within a short interval was beneficial and warrants a larger-scale investigation.

Nakano and colleagues conducted a clinical study to test a PDT + RT combination for Bowen's disease.[40] Four patients (mean age 69.5 years) were treated by PDT with topically administered ALA (20% in an aqueous cream). Illumination was done using an excimer pumped dye laser (λ_{max} = 630 nm) for a total dose of 50 J/cm^2 4−6 h after ALA administration. Within 30 min of PDT, patients were treated with 3 Gy of external beam RT. The combination treatment was repeated 3 more times for a total of 4 PDT + RT sessions. The post-treatment analysis indicated that all lesions disappeared, and no recurrence was observed during the 14-month follow-up period. No significant adverse effects were noted. The success of the treatment was attributed to synergistic interactions between PDT and RT. The authors concluded that a larger scale study is warranted to affirm the observed results and to establish concomitant PDT + RT as a standard treatment option.

4. X-RAY-EXCITABLE SCINTILLATING NANOPARTICLE/PHOTOSENSITIZER CONSTRUCTS FOR CONCOMITANT RADIOTHERAPY AND PHOTODYNAMIC THERAPY

The clinical studies summarized in Table 1 demonstrated that the PDT + RT combination has significant potential in enhancing patient outcomes relative to conventional RT. The clinical data also supported the lack of significant side effects caused by the addition of PDT. The ages of patients tested cover a reasonable range (48−70 years in average/median age), demonstrating a broad potential utility of the PDT + RT approach; note most of these studies were small scale and designed to test the feasibility and safety of the treatment, and therefore, larger-scale studies are warranted to prove efficacy in broad populations. At the same time, these previous studies revealed some limitations of current PDT: (1) the difficulty of complete and uniform illumination of the tumor by light and (2) the difficulty of delivering light into the deep regions of the body (Figure 1). As a solution to address these limitations, the

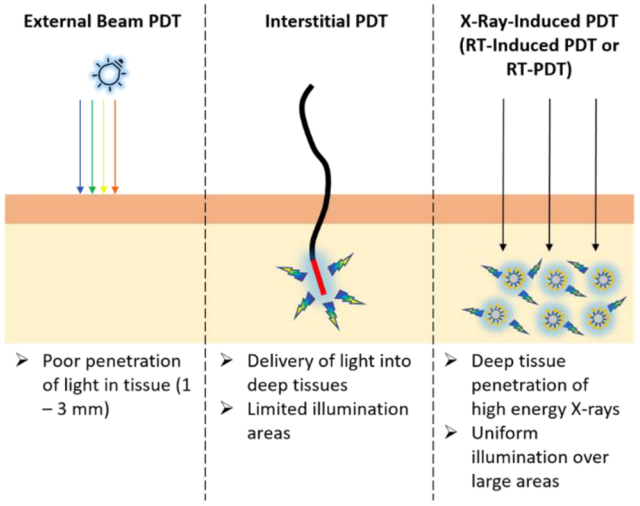

Figure 1. Potential advantages of using X-ray-induced PDT (RT-induced PDT or RT-PDT) relative to conventional external beam/interstitial PDT.

use of scintillating (radioluminescent) nanoparticles (NPs) that can transduce ionizing radiation (such as X-rays) into (UV/visible/IR) light and can thus potentiate radiation-induced PDT (RT-induced PDT or RT-PDT). Various NP constructs, each with nuanced variation in their characteristics, have been demonstrated. An extensive review of initial progress in this area has been reported by Lucky and colleagues.[14] In the remainder of this review, we intend to highlight some of the recent developments that have taken place since this previous review.

A promising approach to implement RT-PDT is to use scintillating (radioluminescent/semiconductor) NPs that interact with incident X-ray photons to produce lower-energy visible light photons that activate nearby photosensitizers. If the energy of the incident X-ray photons is lower than the binding energy of inner-shell electrons (typically < ~500 keV) of the absorber atoms, the so-called photoelectric effect occurs, where the incident photon energy is completely absorbed by an inner-shell electron resulting in the emission of the inner electron and the formation of an inner-shell vacancy.[41−43] This

https://doi.org/10.1021/acsbiomaterials.2c00287
ACS Biomater. Sci. Eng. XXXX, XXX, XXX−XXX

vacancy is subsequently filled by a higher-energy outer-shell electron moving down and releasing a secondary photon and/or an Auger electron. This photoelectric effect is dependent on the atomic number, Z, of the atom, with an increased probability of occurrence with a higher Z. When the incident X-ray photon energy is significantly greater (i.e., on the order of 10^{-1}–10^{0} MeV), an alternative process, called Compton scattering, occurs where the incident photon collides with an outer-shell electron of an atom, resulting in the ejection of the electron and the deflection and a decrease in energy of the original X-ray photon.[41−43] This process is independent of the atomic number of the absorbing material. Both these mechanisms are believed to contribute to the generation of UV/visible light by scintillating NPs under X-ray irradiation and thus the potentiation of RT-PDT.

By using nanoconstructs coloaded with scintillating NPs and photosensitizers (Figure 2), photodynamic effects can be

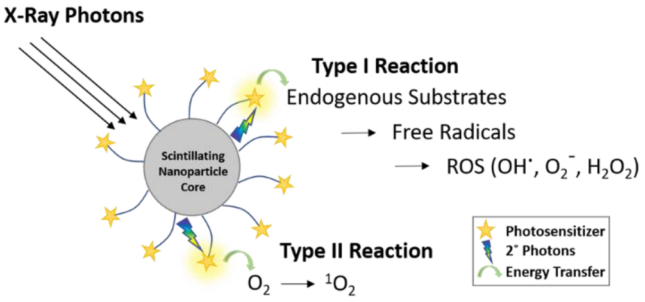

Figure 2. Mechanism of cytotoxic radical generation by nanoscale constructs for RT-PDT. Different photodynamic reactions (type I vs type II) occur depending on photosensitizer type.

produced by X-rays in deep tissues. The optimal distance between the scintillator and the photosensitizer is <10 nm because at such small separation distances, the energy transfer is more efficient; the excitation energy transfer occurs via Förster resonance energy transfer rather than via a less efficient radiation-absorption process.[44] Topics associated with the scintillator-photosensitizer energy transfer mechanisms have recently been reviewed in detail by Cline et al.[44] and Lucky et al.[14] Modern external beam RT (such as intensity modulated RT or IMRT) enables uniform and complete irradiation of a tumor bed with minimal exposure of nearby normal tissue to radiation. Therefore, combined with IMRT, NP-based RT-PDT has the potential to produce localized cytotoxic effects within the tumor. The remainder of this section will highlight notable recent advances in preclinical studies of RT-PDT. Key features of RT-PDT nanoconstructs discussed in this section are also summarized in Table 2.

4.1. Rare-Earth Metal-Doped Semiconductor Nanoparticles. One common approach to achieve the down conversion of X-rays into visible light is to use highly quantum efficient, rare-earth metal-doped semiconductor NPs as scintillators. Along these lines, many NPs have been explored since the first demonstration was published by Chen and coworkers in 2006.[45] These NPs are most often coated with silica to improve colloidal stability and prevent degradation (hydrolysis) of the NPs and the leaching of toxic metal ions into the surroundings. These particles are then further coated with an additional layer of mesoporous silica or polymer material, in which photosensitizer molecules are loaded.

Chen et al.[46] tested rare-earth-doped semiconductor ($LiGa_5O_8$:Cr) NPs in an orthotopic mouse model of NSCLC. $LiGa_5O_8$:Cr NPs have an emission maximum at 720 nm and are thus suitable for activating 2,2-naphthalocyanine, which is a synthetic photosensitizer and has a peak absorbance at 712 nm. The NPs were coated with a layer of amine-functionalized mesoporous silica, into which 2,2-naphthalocyanine was loaded. *N*-Hydroxysuccinimide (NHS) ends of NHS-PEG-COOH chains were reacted with the amine groups of the silica surface under pH 7.4. The carboxyl groups at the other ends of the PEG chains were subsequently conjugated with the amine groups of cetuximab via EDC/NHS coupling for targeting epidermal growth factor receptors (EGFRs), which are overexpressed in many cancer types. In addition to a high luminescence intensity, the formulated NPs (named "NC-LGO:Cr@mSiO_2" NPs) show a strong and persistent afterglow that can be detected by a fluorescence imaging system. Because their afterglow outlasts background luminescence from endogenous fluorophores, the NPs can be used for imaging of deep-seated tumors and thus for guiding RT-PDT. The tumor-targeting and imaging capabilities of the NPs following intravenous administration were validated in an orthotopic mouse model of NSCLC. $^1O_2$ generation by NC-LGO:Cr@mSiO_2 NPs was confirmed by an *in vitro* assay.

A recent study focused on improving the scintillation efficiency of CeF_3 NPs via codoping. Ahmad et al.[47] tested a combination of CeF_3 NPs codoped with Tb^{3+} and Gd^{3+} (scintillator) and rose bengal (RB, photosensitizer (PS)) coencapsulated within a layer of PEGylated-mesoporous silica for treatment of mammary carcinoma. The authors hypothesized that limited *in vivo* success with previous rare-earth NP/PS formulations (such as $CeLaF_3$/LaF_3@chlorin e6, CeF_3@verteporfin, CeF_3@ZnO, and CeF_3:Tb^{3+}@chlorin e6) was due to the low scintillation efficiencies of the NPs and also that codoping of CeF_3 NPs would increase their scintillation efficiency by facilitating an internal energy transfer from Ce^{3+} (activator) to Tb^{3+} (sensitizer), while it would also enable the use of the NPs as an MRI and/or CT contrast agent. An *in vivo* study using mice bearing subcutaneous 4T1 allografts showed that RT-PDT was significantly more therapeutically effective than treatment with X-rays alone; experiments were performed at 2 different X-ray doses (3 and 6 Gy). However, this study did not include control groups treated with undoped or singly doped CeF_3 NPs for comparison with the codoped NPs. Metabolomic analysis of serum suggested that a down-regulation of precursors for protein/DNA synthesis was responsible for tumor destruction. A biodistribution study indicated that the NPs initially accumulated in the liver, spleen, and lungs, but were cleared from the body within 30 days without causing any significant toxicity. Overall, it was concluded that concurrent NP treatment significantly improved efficacy relative to RT alone.

Jiang et al.[48] reported an alternative, codoped NP-based RT-PDT strategy which used RT-PDT in combination with antiangiogenic therapy (AAT) (Figure 3). CaF_2:3%Ce^{3+},1% Tb^{3+} (CCT) NPs and sunitinib (SU, a small molecule inhibitor of multiple receptor tyrosine kinases) were coloaded into polyamidoamine (PAMAM) dendrimers, which resulted in the formation of a dual-core−satellite structure. Hydrophilic PEG chains and RB photosensitizer moieties were covalently grafted to the surface of the NP/SU-loaded dendrimers. This nanoconstruct generated a significant level of $^1O_2$ under low dose X-ray irradiation (1 Gy), resulting in necrotic cell death *in*

https://doi.org/10.1021/acsbiomaterials.2c00287
ACS Biomater. Sci. Eng. XXXX, XXX, XXX−XXX

Table 2. Summary of Nanoparticle Constructs Discussed in this Review

Photosensitizer	Peak Absorbance (nm)	Scintillator/Energy Transducer	Peak Emission (nm)	Encapsulation Method	Diameter (nm)	Cellular Target	Targeting Moiety	ROS Type	Cell Death Mechanism	Ref
2,2-Naphthalocyanine	712	$LiGa_5O_8$:Cr	720	Mesoporous SiO_4 with PEG chains	~130	EGFR	Cetuximab	$^1O_2$	N/A	46
Rose Bengal	540	CeF_3:Gd^{3+},Tb^{3+}	542	Mesoporous SiO_4 with PEG chains	89.2	N/A	N/A	$^1O_2$	N/A	47
Rose Bengal	540	CaF_2:Ce^{3+},Tb^{3+}	542	PAMAM dendrimers covalently linked with RB moieties	65.3	N/A	N/A	$^1O_2$	Necrosis/ apoptosis	48
Verteporfin	410	Au	N/A	HS-PEG and HS-PEG-NH_2	N/A	N/A	N/A	$^1O_2$	N/A	49
Verteporfin	410	Au	N/A	PLGA	160	Mitochondria	Triphenylphosphonium bromide	$^1O_2$	Apoptosis	50
Rose Bengal	570	Glutathione-coated Au clusters	570	Poly(allylamine hydrochloride)	65.6	Cell membrane and DNA	RGD Peptide	$^1O_2$ and•OH	N/A	51
Bilirubin	450	$CaWO_4$	420/500	PEG-bilirubin	180	N/A	N/A	$^1O_2$	Necrosis/ apoptosis	55
TCPP	414	Hf	N/A	PEG	130	DNA	N/A	$^1O_2$	N/A	58
$Ir[bpy(ppy)_2]^+$ or $[Ru(bpy)_3]^{2+}$	355 and 450, respectively	$Hf_6O_4(OH)_4(HCO_2)_6$	N/A	N/A	500	DNA	N/A	$^1O_2$	N/A	62
Cu-Cy	360	Cu-Cy	607	Coated with pH-low insertion peptide	200	N/A	pH-low insertion peptide	$^1O_2$	Apoptosis/ necrosis	61
Ag_3PO_4	295	$LiLuF_4$:Ce	305/235	SiO_4	200−1000	DNA	N/A	•OH	Apoptosis/ mitotic death	64
TiO_2	~290	FDG	N/A	TF-TC	108	Cell membrane and DNA	TF	•OH and $O_2^{\bullet-}$	Necrosis/ apoptosis	66
TiO_2	~290	^{68}Ga-BSA	N/A	Dopamine-conjugated carboxymethyl dextran sodium salt	98.7	DNA	Dextran	•OH and $O_2^{\bullet-}$	N/A	67
TCPP	400	^{89}Zr	N/A	DSPE-PEG	89.9	N/A	$(Zn_{0.4}Mn_{0.6})Fe_2O_4$ NPs (magnetic targeting)	$^1O_2$	Apoptosis	68
NH_2-$Ti_{32}O_{16}$ nanoclusters	250−300	FDG	N/A	PEG	4	DNA	Dopamine	•OH	Apoptosis	69

https://doi.org/10.1021/acsbiomaterials.2c00287
ACS Biomater. Sci. Eng. XXXX, XXX, XXX−XXX

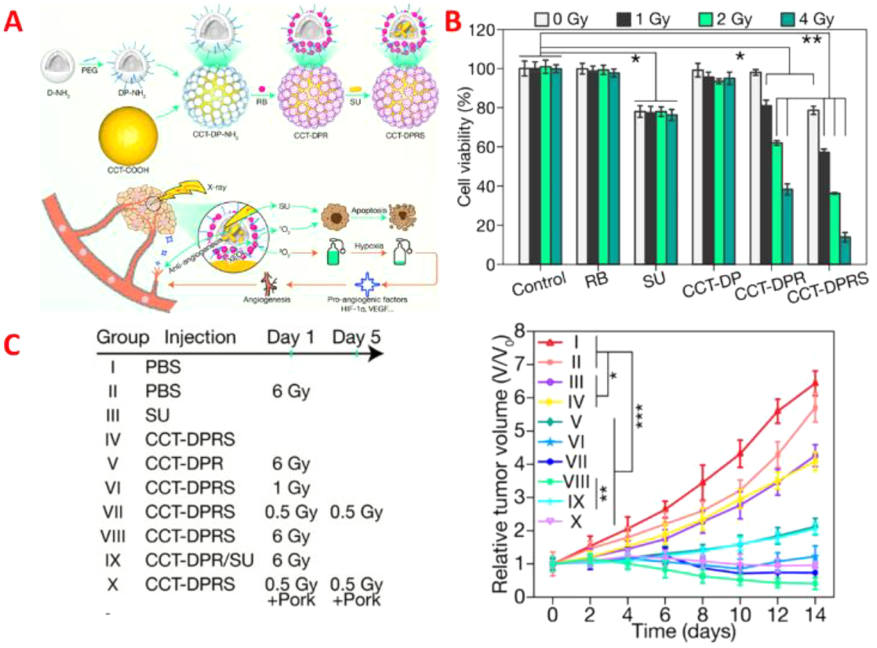

Figure 3. (A) Formulation of CaF_2:3%Ce^{3+}:1%Tb^{3+} NPs grafted with rose bengal-conjugated PEG dendrimer and coloaded with Sunitinib (CCT-DPRS) proposed for concomitant RT-PDT and antiangiogenic therapy. (B) *In vitro* cell viability assay conducted in 4T1 cells (N = 5). (C) *In vivo* tumor suppression assay conducted in mice bearing subcutaneously implanted 4T1 tumors (N = 5). Reproduced with permission from ref 48. Copyright 2021 American Chemical Society.

vitro. Further, SU released from the dendrimers inhibited capillary-like tube formation in a human umbilical vein cell line, validating its antiangiogenic effect. In a subcutaneous 4T1 mouse tumor model, RT-PDT alone reduced the tumor volume (tumor growth inhibition ratio measured at 14 days (TGI) = 79%). When combined with the antiangiogenic impact of SU, the RT-PDT suppressed tumor growth to a much greater extent (TGI = 112%). Interestingly, in this RT-PDT-AAT therapy, 2 doses of 0.5 Gy delivered 4 days apart produced a better therapeutic result than 6 Gy delivered in a single fraction, which was attributed to the tumor reoxygenation effect that occurred in the dose fractionated situation. No indication of toxicity was observed in organs of mice treated with the nanoconstruct. The authors concluded that the RT-PDT-AAT is a promising strategy that warrants further mechanistic/toxicological investigation.

4.2. Metal/Metal Oxide Nanoparticles. Metal NPs have also been used for RT-PDT applications. Gold (Au) NPs have received a lot of attention because of their relative safety and the ease with which their surface can be functionalized with photosensitizing moieties.[49] A recent example is Au NPs functionalized with verteporfin (VP),[49] which is an FDA-approved PS for PDT of neovascular macular degeneration. VP has an intense absorption at 365 nm and a weaker absorption at 700 nm. However, unlike ordinary photosensitizers, VP causes the formation of $^1O_2$ under direct X-ray exposure. Au NPs enhance this effect by strengthening the electric field near their surface, which increases the absorption of radiation by VP. Clement et al. investigated the efficacy and safety of using SH-PEG/SH-PEG-NH_2-functionalized Au NPs for X-ray-induced PDT *in vitro*.[49] The same group also investigated the use of triphenylphosphonium (TPP)-functionalized biodegradable PLGA capsules coloaded with VP and Au NPs to produce X-ray-induced PDT effects in mice bearing colorectal cancer xenografts.[50] In the presence of these NPs, a 4 Gy dose of X-rays produced a therapeutic effect equivalent to 12 Gy of X-rays without the NPs, while the NPs did not produce any side effects. TPP functionalization enabled mitochondrial targeting, leading to cell death via apoptosis. Considering that PLGA and VP are already FDA-approved, and Au NPs are minimally toxic, the authors argued that this technology has the potential for clinical translation.

Another example of using Au NP constructs was reported by Sun and co-workers.[51] It had previously been known that protein-protected Au clusters exhibit optical luminescence under X-ray irradiation. Taking advantage of this property, glutathione-protected Au atomic clusters of ∼68 nm diameter (named "aggregation-induced emission heterogeneous Au (AIE-Au) clustoluminogens") were used as an energy transducer for RB-mediated PDT under X-ray activation. AIE-Au clustoluminogens themselves act as a radiosensitizer by producing secondary electrons and eventually hydroxyl radicals under X-ray irradiation.[52] Due to these dual mechanisms, AIE-Au clustoluminogens were shown to be able to improve the effectiveness of X-ray treatment even at as little as 1 Gy dose in multiple radio-resistant cell lines (including U87MG, HEPG2, and PC3) both *in vitro* and *in vivo*. Mechanistic investigation revealed that cellular damage occurred mainly due to peroxidation of the lipids in the cellular membrane in addition to direct DNA breakage. It was also demonstrated that AIE-Au clustoluminogens enhance contrast for CT/fluorescence imaging, which makes them a good candidate for theranostic/theragnostic applications.

Alternatively to metal NPs, our laboratory has been exploring the possibility of using nontoxic $CaWO_4$ NPs as a potentiator for RT-PDT because $CaWO_4$ is a radioluminescent/scintillating (semiconducting metal oxide) material which emits UV-A/blue light under X-ray irradiation.[53,54] A poly(ethylene glycol)-bilirubin (PEG-BR)-encapsulated $CaWO_4$ NP formulation has been developed (Figure 4).[55] Secondary

https://doi.org/10.1021/acsbiomaterials.2c00287
ACS Biomater. Sci. Eng. XXXX, XXX, XXX−XXX

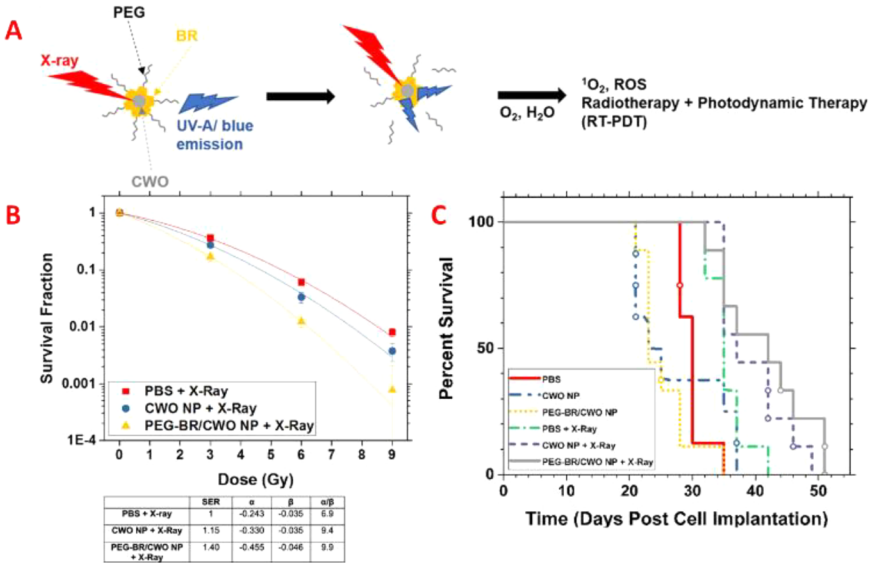

	SER	α	β	α/β
PBS + X-ray	1	-0.243	-0.035	6.9
CWO NP + X-Ray	1.15	-0.330	-0.035	9.4
PEG-BR/CWO NP + X-Ray	1.40	-0.455	-0.046	9.9

Figure 4. (A) Radiotherapy enhancement mechanism of PEGylated-bilirubin/$CaWO_4$ NPs (PEG-BR/CWO NPs). (B) *In vitro* clonogenic cell survival assay conducted in HN31 cells ($N = 3$). Table summarizes SERs (estimated at 10% cell survival) and α/β ratios (where α and β are linear-quadratic model parameters). (C) Kaplan–Meier curves from an *in vivo* survival assay conducted using mice bearing subcutaneously implanted HN31 tumors. Mice were irradiated with 8 Gy X-rays delivered in 4 fractions of 2 Gy/day ($N = 9$). Reproduced with permission from ref 55. Copyright 2020 American Chemical Society.

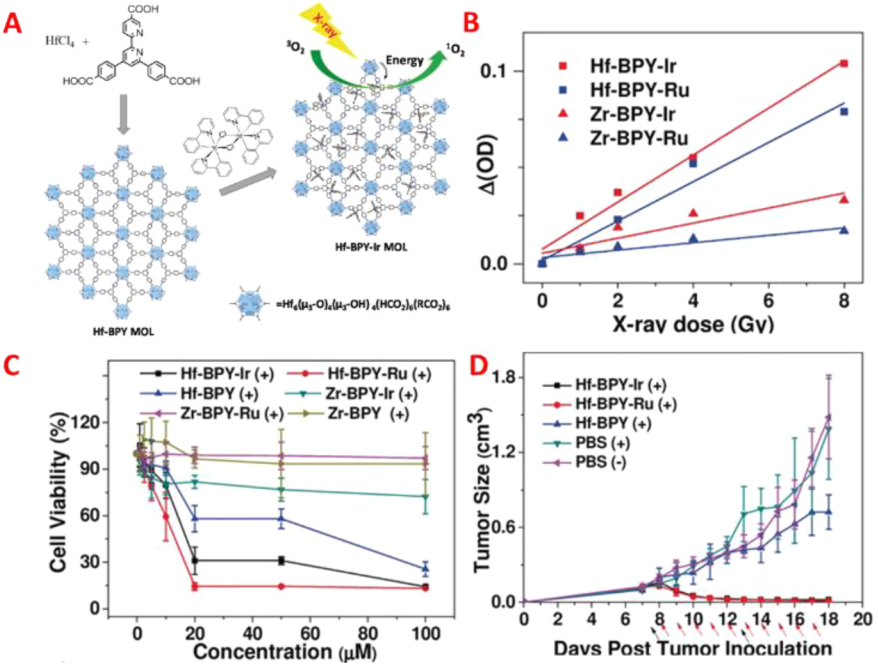

Figure 5. (A) Synthesis and mechanism of action of Hf-based metal–organic layers (MOLs). (B) *In vitro* $^1O_2$ production of MOLs at different X-ray doses. (C) *In vitro* cell viability assay conducted in MC38 cells upon 2 Gy X-ray irradiation ($N = 6$). (D) *In vivo* tumor suppression assay conducted in mice bearing subcutaneously implanted MC38 tumors. Mice were irradiated with 10 Gy X-rays delivered in 10 fractions of 1 Gy/day ($N = 4$). Reproduced with permission from ref 59. Copyright 2017 John Wiley & Sons.

UV-A/blue light generated by $CaWO_4$ NPs under X-ray irradiation is absorbed by BR which serves as a photosensitizer. Photoactivated BR produces cytotoxic singlet oxygen ($^1O_2$) molecules. In radio-resistant (p53 mutant) HN31 (head and neck squamous cell carcinoma) cells, a sensitization enhancement ratio (SER) of 1.4 was achieved with 320 keV X-rays, while no cytotoxicity of the NPs was observed *in vitro*. Efficacy of concurrent $CaWO_4$ NPs with X-ray radiation was validated *in vivo* in a mouse HN31 xenograft model.[55] Histopathological analysis confirmed that $CaWO_4$ NPs do not damage major organs following intratumoral administration and enhance necrosis within the tumors.[55] Other variants of the $CaWO_4$ NP formulation have also been tested and shown to be effective in enhancing the effectiveness of X-rays.[53,56] When compared with rare-earth metal-based semiconductor/scintillating NPs,

https://doi.org/10.1021/acsbiomaterials.2c00287
ACS Biomater. Sci. Eng. XXXX, XXX, XXX–XXX

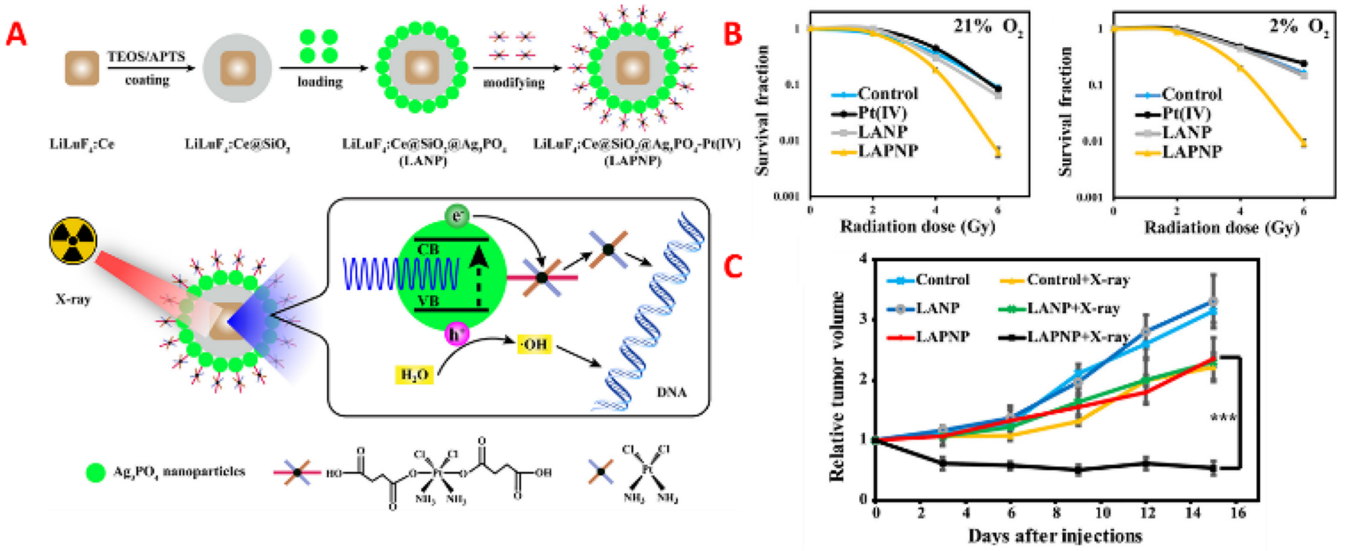

Figure 6. (A) Formulation and mechanism of action of $LiLuF_4$:Ce@SiO_2@ Ag_3PO_4@Pt(IV) NPs (LAPNPs). (B) *In vitro* clonogenic cell survival assay conducted in HeLa cells under normoxic and hypoxic conditions (N = 3). (C) *In vivo* tumor suppression assay conducted in mice bearing subcutaneously implanted HeLa tumors. Mice were irradiated with 4 Gy X-rays (N = 5). Reproduced with permission from ref 64. Copyright 2018 American Chemical Society.

$CaWO_4$ is potentially advantageous in terms of biosafety and an abundance of the raw chemicals.

4.3. Nanoscale Metal−Organic Frameworks. Metal−organic frameworks (MOFs) are formed by self-assembly of metal ions with organic linkers (polydentate ligands). Recently, nanoscale MOFs (MOF NPs) have been successfully synthesized.[57] Various anticancer agents and photosensitizers have been loaded into MOF NPs. Various combinations of different types of metal centers and organic linkers have also been demonstrated. Liu et al. developed nanoscale MOFs composed of Hf^{4+} ions and tetrakis(4-carboxyphenyl)-porphyrin (TCPP) photosensitizer linkers.[58] The high-Z Hf atoms efficiently absorbs high-energy X-rays and subsequently transfers the X-ray energy to the photosensitizers. This was the first-reported use of MOFs for RT-PDT. These MOF NPs were further PEGylated (via coating with PEG-grafted poly(maleicanhydride-*alt*-1-octadecene)) to enhance stability against aggregation. The MOF NPs significantly improved the effect of radiation (6 Gy X-rays) on 4T1 cancer cells *in vivo*, while no significant toxicity was observed over 30 days post-IV administration in mice. The same group further demonstrated that 2D MOF nanosheets (metal−organic layers or MOLs) produce greater therapeutic effects than their 3D analogues because singlet oxygen molecules generated under X-ray irradiation can be released easier from the 2D structure (Figure 5).[59] MOL NPs were constructed using $Ir[bpy-(ppy)_2]^+$ or $[Ru(bpy)_3]^{2+}$-derived tricarboxylate photosensitizing ligands, benzene-1,3,5-tribenzoate linkers, and $[Hf_6O_4(OH)_4(HCO_2)_6]$ secondary building units. These MOLs generate $^1O_2$ under X-ray irradiation because the Hf atoms directly transfer the X-ray energy to the PS compounds. The concomitant MOL NP + X-ray (10 Gy delivered in 10 fractions of 1 Gy dose, 120 kVp) treatment caused an 82.3% and 90.1% reduction in tumor volume in mice bearing colon adenocarcinoma for Ir- and Ru-based photosensitizers, respectively. No toxicity due to MOL NPs was detected in histological sections of organs. Currently, a company (RiMO Therapeutics) is conducting a Phase I clinical trial on this technology.[60]

5. DEVELOPMENT OF DIRECTLY X-RAY-ACTIVATABLE PHOTOSENSITIZERS

Alternatively to using X-ray energy transducers (scintillating NPs), efforts have also been made to develop photosensitizers that can be directly activated by X-rays. A potential advantage of this approach is that X-ray's ROS generation efficiency can be improved by bypassing the photon energy transfer (i.e., scintillation) step.

Ma et al.[61] developed a Cu-cysteamine (Cu-Cy) complex ($Cu_3Cl(SR)_2$ where R = $CH_2CH_2NH_2$), in which both thiol and amine groups bind to Cu^+ ions, unlike conventional complexes in which only thiols bind to Cu. This newer architecture enables more efficient radioluminescence emission and direct $^1O_2$ production under X-ray irradiation relative to other Cu-Cy complexes. *In vitro* experiments in colorectal cancer cells indicated that $Cu_3Cl(SR)_2$ enhances the effect of X-rays (2−3 Gy, 90 kV) by 40−60%.[62] This enhancement was attributed to the accumulation of the complexes in the mitochondria, which led to increased apoptosis/necrosis. In a follow-up study, $Cu_3Cl(SR)_2$ NPs were functionalized with pH-low insertion peptides for targeting to low pH cancer cells. The efficacy of these NPs was validated in mice bearing murine breast tumors.[63]

The majority of photosensitizers studied produce cytotoxicity via generation of $^1O_2$, which makes them reliant on the availability of molecular oxygen. As an oxygen-independent alternative, Wang et al. proposed the use of photocatalytic semiconductor NPs capable of lysing water into cytotoxic •OH (Figure 6).[64] Their photosensitizer system is composed of a $LiLuF_4$:Ce core and a silica shell loaded with Ag_3PO_4 NPs and functionalized with cisplatin prodrugs (Pt(IV) complexes). The photosensitization mechanism is as follows: $LiLuF_4$:Ce absorbs X-rays and emits UVB/UVA light (305/325 nm). Ag_3PO_4 NPs (peak absorbance at 295 nm) absorb UV light, which results in the formation of electron−hole pairs. The

https://doi.org/10.1021/acsbiomaterials.2c00287
ACS Biomater. Sci. Eng. XXXX, XXX, XXX−XXX

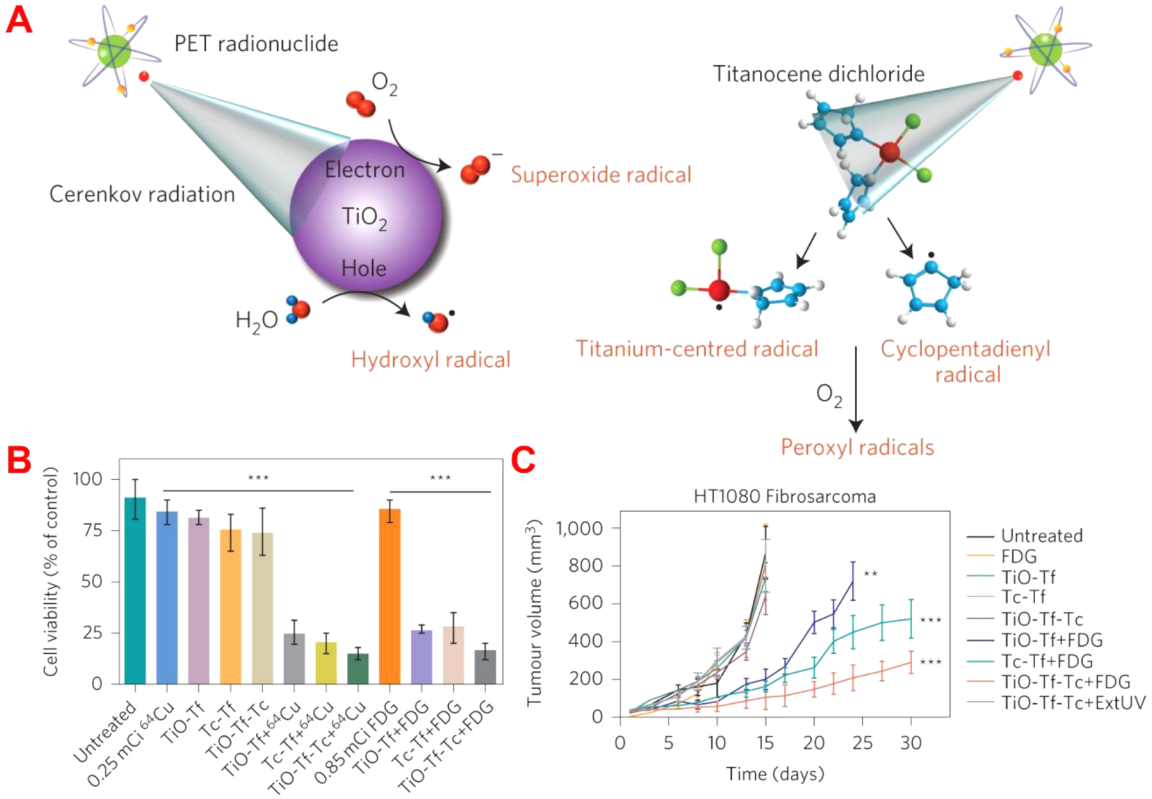

Figure 7. (A) A schematic explaining the mechanism of Cherenkov radiation-induced PDT. (B) Cell kill efficacy of TiO_2 NPs under the influence of FDG in HT1080 cells *in vitro* ($N = 3$). (C) Tumor growth suppression by TiO_2 NPs under the influence of FDG in mice bearing subcutaneous HT1080 tumors *in vivo* ($N = 6$). Reproduced with permission from ref 66. Copyright 2015 Springer Nature.

majority of these electron−hole pairs recombine. However, Pt(IV) acts as a sacrificial electron acceptor, leaving unpaired holes which catalyze photolysis of water into hydroxyl free radicals. Upon accepting electrons, Pt(IV) converts into cisplatin which is an anticancer agent capable of causing DNA damage. This mechanism was validated to be operative under both normoxic and hypoxic conditions, whereas formulations devoid of Pt(IV) produced hydroxyl radicals only under normoxic conditions. In *in vitro* clonogenic assays, the sensitization enhancement ratios were determined to be 1.24 and 1.28, respectively, under normoxic and hypoxic conditions. This radiosensitization effect was attributed to increased DNA damage, which caused increased apoptosis and proliferative dysfunction (mitotic catastrophe). In mice bearing HeLa cells, concomitant NPs caused near complete tumor suppression. No significant toxicity was observed in histological analysis of major organs.

6. CHERENKOV (CERENKOV) RADIATION-INDUCED PHOTODYNAMIC THERAPY

Alternative approaches have also been developed that do not rely on external-beam radiation but instead take advantage of the UV/visible Cherenkov radiation produced when a charged particle travels inside a dielectric medium at a speed greater than the speed of light.[65] An advantage is that clinical positron emission tomography (PET) radionuclides can be used as the radiation source. The concept was pioneered by Achilefu and co-workers, who used radiolabeled 2′-deoxy-2′-(^{18}F)fluoro-D-glucose (FDG) as the UV emitter to potentiate the photocatalytic activity of TiO_2 NPs (Figure 7).[66] Upon absorbing UV light, type I photodynamic reactions occur in which electron−hole pairs are generated within TiO_2 which cause catalytic degradation of chemisorbed H_2O molecules into cytotoxic •OH and $O_2^{\bullet-}$ radicals. Concomitant IV administration of TiO_2 NPs functionalized with apo-transferrin (TF) (for colloidal stability and tumor targeting) and titanocene (TC) (for radical generation) produced significant tumor regression in mouse HT1080 (fibrosarcoma) xenografts and also a significant delay in tumor growth in mouse A549 (NSCLC) xenografts. Because of the tumor specificity of both the radionucleotides and NPs, no toxicity was observed in excretory organs (i.e., kidneys and liver).

After this initial success, efforts have been directed at using radioisotopes with greater luminescence. Duan et al. proposed that ^{68}Ga-bovine serum albumin (^{68}Ga-BSA) is advantageous over ^{18}F-based radionucleotides (e.g., FDG) because it has a 30-fold higher photon yield.[67] Typically, PDT requires 10−30 times higher doses of ^{18}F compared with PET imaging. Therefore, with ^{68}Ga, it becomes possible to perform PDT (via activation of the TiO_2 photocatalyst) at much lower ^{68}Ga doses (i.e., at doses needed for diagnostic imaging). In this study, TiO_2 NPs were coated with dextran for colloidal stability and tumor specificity. Despite its significantly lower uptake by 4T1 cells (1.1% for ^{68}Ga-BSA vs 6.35% for FDG), ^{68}Ga-BSA produced 4.5-times more amount of photons and correspondingly greater cell killing. The same trend was also verified in mouse 4T1 allografts treated with intratumorally injected ^{68}Ga-BSA and TiO_2 NPs. ^{68}Ga is also currently clinically used. No side effects were observed with ^{68}Ga-BSA and TiO_2 NPs.

Ni et al. developed a radionuclide/photosensitizer nanoconstruct consisting of $(Zn_{0.4}Mn_{0.6})Fe_2O_4$ NPs (MNPs)

https://doi.org/10.1021/acsbiomaterials.2c00287
ACS Biomater. Sci. Eng. XXXX, XXX, XXX−XXX

functionalized with DSPE-PEG (stabilizing agent), meso-TCPP (photosensitizer), and ^{89}Zr (radioisotope).[68] The focus of the study was to improve tumor targeting by using the magnetic properties of MNPs. In mice bearing 4T1 tumors in both flanks, an external magnetic field was applied to one tumor but not the other. The magnetic field induced an increased accumulation of MNPs in the tumor. Although ^{89}Zr has a lower photon yield than ^{68}Ga (2.29 vs 33.90 photons/decay/mm, respectively), ^{89}Zr has a much longer radioactive half-life (78.4 h) than ^{68}Ga (67.7 min). Therefore, the Cherenkov luminescence was able to produce sustained TCPP photosensitization and accordingly sustained $^1O_2$ generation. The tumors treated with MNPs under the magnetic field were nearly completely suppressed for 2 weeks, whereas the nonmagnetically exposed tumors (control) showed little effect of the MNP treatment. Histopathological analysis showed no significant organ damage except to the liver; the damaged liver recovered within 2 months.

Li and co-workers used NH_2-$Ti_{32}O_{16}$ nanoclusters (~ 4 nm diameter) as a type I photosensitizer,[69] which has a greater photocatalytic activity than TiO_2 NPs and also causes an increased chemodynamic effect. Chen et al. tested several common photosensitizers for use with FDG in Cherenkov radiation-induced PDT and identified vertoporfin as the best choice.[70] While radionuclides have an innate ability to emit UV,[71] their own cell kill effects are not comparable with that of external beam RT. Thus, Cherenkov-induced PDT is unable to produce the synergistic effects of PDT and RT. On the other hand, using clinical radionuclides offers a unique opportunity to combine therapy and diagnosis.

7. CONCLUDING REMARKS: GAPS IN CURRENT KNOWLEDGE

PDT is an effective local therapy, well tolerated, and facile. Using PDT in combination with RT results in improved prognosis relative to RT alone. However, there are limitations of PDT with the most important one being the difficulty of uniform illumination of the entire tumor which limits the efficacy of PDT. Various novel scintillator/photosensitizer constructs that use X-rays (instead of visible light) as the triggering mechanism for PDT have been developed to address this issue. Several prominent examples of such "RT-PDT" approaches have been reviewed, including rare-earth metal-doped semiconductors, metal/metal oxide semiconductors, metal−organic frameworks, X-ray activatable photosensitizers, and oxygen-independent photosensitizers. In addition, recent progress in Cherenkov radiation-induced PDT is also highlighted.

For clinical translation of RT-PDT, there are gaps that need to be filled. The efficacy of RT-PDT depends on delivery and distribution of NPs within the tumor tissue. Thus far, all preclinical proof-of-concept studies have been performed using cell line-based mouse tumor models; it is uncertain whether similar success can be achieved with spontaneous tumors characterized by more complex tissue/vascular structures and correspondingly higher barriers for NP transport. Strategies for improving intratumoral distribution of NPs need to be developed.

Preclinical studies of RT-PDT are typically performed using X-rays having energies of tens to hundreds of keV, whereas clinical RT typically uses beams of megavoltage X-ray photons. This difference in photon energy is expected to cause a shift in the dominant mechanism of interaction between the incident photon and the tumor tissue and also between the incident photon and the NP; both the relative biological effectiveness of X-ray beams itself[72] and the energy absorption by the NP[52] are decreasing functions of the incident photon energy. Therefore, preclinical studies with low-energy benchtop irradiators tend to give an overestimation of the effect of the therapy. Further preclinical validation of the performance of NP candidates[52,73] under clinical photon energy conditions (e.g., 6 MeV) would be necessary before moving on to the next stage of the development.

Rare-earth metal-doped semiconductor NPs have been most commonly studied for their potential use in RT-PDT. Because of their high quantum yields, these materials have shown impressive efficacies in tumor models *in vivo*. However, currently there is lack of data on the long-term chemical stability and toxicity of these materials. For instance, lanthanide NPs, such as those containing cerium, have been shown to cause toxicity to brain and liver.[74] Free gadolinium ions (Gd^{3+}) are highly toxic, although their toxicity is reduced upon chelation.[75] The long-term safety and bioresorbability/biopersistence characteristics are essential information for evaluating the clinical feasibility of these materials. Consideration of these regulatory issues early on, i.e., even during the discovery stage, would make research efforts more potentially impactful. Overall, RT-PDT is a promising concept for high localized and efficient treatment of solid tumors, and nanotechnology will continue to play a central role in advancing this vision.

AUTHOR INFORMATION

Corresponding Author

You-Yeon Won − *Davidson School of Chemical Engineering, Purdue University, West Lafayette, Indiana 47907, United States; Purdue University Center for Cancer Research, West Lafayette, Indiana 47906, United States;* orcid.org/0000-0002-8347-6375; Email: yywon@purdue.edu

Author

Dhushyanth Viswanath − *Davidson School of Chemical Engineering, Purdue University, West Lafayette, Indiana 47907, United States*

Complete contact information is available at: https://pubs.acs.org/10.1021/acsbiomaterials.2c00287

Notes

The authors declare no competing financial interest.

ACKNOWLEDGMENTS

Funding for this research was provided by Purdue University Center for Cancer Research (PCCR, P30CA023168, DDMS Collaborative Ideas Project), Purdue University Discovery Park (Walther Oncology Physical Sciences and Engineering Research Embedding Program), Lodos Theranostics LLC (Gift Grant), and the Davidson School of Chemical Engineering at Purdue University. Y.Y.W. is also grateful for funding from NSF (CBET-1803968) and D.V. for the Leslie Bottorff Fellowship from Purdue University.

REFERENCES

(1) Siegel, R. L.; Miller, K. D.; Jemal, A. Cancer statistics, 2019. *CA: A Cancer Journal for Clinicians* **2019**, *69* (1), 7−34.

(2) Miller, K. D.; Siegel, R. L.; Lin, C. C.; Mariotto, A. B.; Kramer, J. L.; Rowland, J. H.; Stein, K. D.; Alteri, R.; Jemal, A. Cancer treatment

and survivorship statistics, 2016. *CA: A Cancer Journal for Clinicians* **2016**, *66* (4), 271−289.
(3) Miller, K. D.; Nogueira, L.; Mariotto, A. B.; Rowland, J. H.; Yabroff, K. R.; Alfano, C. M.; Jemal, A.; Kramer, J. L.; Siegel, R. L. Cancer treatment and survivorship statistics, 2019. *CA: A Cancer Journal for Clinicians* **2019**, *69* (5), 363−385.
(4) Hidalgo, M.; Cascinu, S.; Kleeff, J.; Labianca, R.; Löhr, J. M.; Neoptolemos, J.; Real, F. X.; Van Laethem, J.-L.; Heinemann, V. Addressing the challenges of pancreatic cancer: Future directions for improving outcomes. *Pancreatology* **2015**, *15* (1), 8−18.
(5) Arnal, M. J. D.; Arenas, Á. F.; Arbeloa, Á. L. Esophageal cancer: Risk factors, screening and endoscopic treatment in Western and Eastern countries. *World journal of gastroenterology: WJG* **2015**, *21* (26), 7933−7943.
(6) Thariat, J.; Hannoun-Levi, J.-M.; Myint, A. S.; Vuong, T.; Gérard, J.-P. Past, present, and future of radiotherapy for the benefit of patients. *Nature reviews Clinical oncology* **2013**, *10* (1), 52−60.
(7) Bryant, A. K.; Banegas, M. P.; Martinez, M. E.; Mell, L. K.; Murphy, J. D. Trends in radiation therapy among cancer survivors in the United States, 2000−2030. *Cancer Epidemiology and Prevention Biomarkers* **2017**, *26* (6), 963−970.
(8) Citrin, D. E. Recent Developments in Radiotherapy. *New England Journal of Medicine* **2017**, *377* (11), 1065−1075.
(9) Housman, G.; Byler, S.; Heerboth, S.; Lapinska, K.; Longacre, M.; Snyder, N.; Sarkar, S. Drug Resistance in Cancer: An Overview. *Cancers* **2014**, *6* (3), 1769−1792.
(10) Kim, B. M.; Hong, Y.; Lee, S.; Liu, P.; Lim, J. H.; Lee, Y. H.; Lee, T. H.; Chang, K. T.; Hong, Y. Therapeutic Implications for Overcoming Radiation Resistance in Cancer Therapy. *International Journal of Molecular Sciences* **2015**, *16* (11), 26880−26913.
(11) Janssen, E. M.; Dy, S. M.; Meara, A. S.; Kneuertz, P. J.; Presley, C. J.; Bridges, J. F. P. Analysis of Patient Preferences in Lung Cancer - Estimating Acceptable Tradeoffs Between Treatment Benefit and Side Effects. *Patient Prefer Adherence* **2020**, *14*, 927−937.
(12) Eliasson, L.; de Freitas, H. M.; Dearden, L.; Calimlim, B.; Lloyd, A. J. Patients' Preferences for the Treatment of Metastatic Castrate-resistant Prostate Cancer: A Discrete Choice Experiment. *Clinical Therapeutics* **2017**, *39* (4), 723−737.
(13) Dolmans, D.; Fukumura, D.; Jain, R. K. TIMELINE: Photodynamic therapy for cancer. *Nature Reviews Cancer* **2003**, *3*, 380−387.
(14) Lucky, S. S.; Soo, K. C.; Zhang, Y. Nanoparticles in photodynamic therapy. *Chem. Rev.* **2015**, *115* (4), 1990−2042.
(15) Chilakamarthi, U.; Giribabu, L. Photodynamic Therapy: Past, Present and Future. *Chem. Rec* **2017**, *17* (8), 775−802.
(16) Brown, S. B.; Brown, E. A.; Walker, I. The present and future role of photodynamic therapy in cancer treatment. *Lancet Oncol* **2004**, *5* (8), 497−508.
(17) Allison, R. R.; Moghissi, K. *Oncologic photodynamic therapy: Clinical strategies that modulate mechanisms of action.* **2013**, *10* (4), 331−341.
(18) Meyer-Betz, F. Untersuchungen über die biologische (photodynamische) Wirkung des Hämatoporphyrins und anderer Derivate des Blut-und Gallenfarbstoffs. *Dtsch. Arch. Klin. Med.* **1913**, *112* (476−450), 0366−8576.
(19) Figge, F. H. J.; Weiland, G. S.; Manganiello, L. O. J. Cancer Detection and Therapy. Affinity of Neoplastic, Embryonic, and Traumatized Tissues for Porphyrins and Metalloporphyrins. *Proceedings of the Society for Experimental Biology and Medicine* **1948**, *68* (3), 640−641.
(20) Schwartz, S.; Absolon, K.; Vermund, H. Some relationships of porphyrins, X-rays and tumors. *Univ. Minn. Med. Bull.* **1955**, *27*, 1−37.
(21) Dougherty, T. J.; Grindey, G. B.; Fiel, R.; Weishaupt, K. R.; Boyle, D. G. Photoradiation therapy. II., Cure of animal tumors with hematoporphyrin and light. *Journal of the National Cancer Institute* **1975**, *55* (1), 115−121.
(22) Dougherty, T. J.; Kaufman, J. E.; Goldfarb, A.; Weishaupt, K. R.; Boyle, D.; Mittleman, A. Photoradiation Therapy for the Treatment of Malignant Tumors. *Cancer Res.* **1978**, *38* (8), 2628−2635.
(23) Shafirstein, G.; Bellnier, D.; Oakley, E.; Hamilton, S.; Potasek, M.; Beeson, K.; Parilov, E. Interstitial photodynamic therapy—a focused review. *Cancers* **2017**, *9* (2), 12.
(24) Baskaran, R.; Lee, J.; Yang, S.-G. Clinical development of photodynamic agents and therapeutic applications. *Biomaterials Research* **2018**, *22* (1), 25.
(25) Eriksson, D.; Stigbrand, T. Radiation-induced cell death mechanisms. *Tumor Biology* **2010**, *31* (4), 363−372.
(26) Skvortsova, I.; Debbage, P.; Kumar, V.; Skvortsov, S. Radiation resistance: Cancer stem cells (CSCs) and their enigmatic pro-survival signaling. *Seminars in Cancer Biology* **2015**, *35*, 39−44.
(27) Grebeňová, D.; Kuželová, K.; Smetana, K.; Pluskalová, M.; Cajthamlová, H.; Marinov, I.; Fuchs, O.; Souček, J.; Jarolım, P.; Hrkal, Z. Mitochondrial and endoplasmic reticulum stress-induced apoptotic pathways are activated by 5-aminolevulinic acid-based photodynamic therapy in HL60 leukemia cells. *Journal of Photochemistry and Photobiology B: Biology* **2003**, *69* (2), 71−85.
(28) Ji, Z.; Yang, G.; Vasovic, V.; Cunderlikova, B.; Suo, Z.; Nesland, J. M.; Peng, Q. Subcellular localization pattern of protoporphyrin IX is an important determinant for its photodynamic efficiency of human carcinoma and normal cell lines. *Journal of Photochemistry and Photobiology B: Biology* **2006**, *84* (3), 213−220.
(29) Kriska, T.; Korytowski, W.; Girotti, A. W. Role of mitochondrial cardiolipin peroxidation in apoptotic photokilling of 5-aminolevulinate-treated tumor cells. *Arch. Biochem. Biophys.* **2005**, *433* (2), 435−446.
(30) Noodt, B. B.; Berg, K.; Stokke, T.; Peng, Q.; Nesland, J. M. Apoptosis and necrosis induced with light and 5-aminolaevulinic acid-derived protoporphyrin IX. *Br. J. Cancer* **1996**, *74* (1), 22−29.
(31) Tan, I. B.; Dolivet, G.; Ceruse, P.; Poorten, V. V.; Roest, G.; Rauschning, W. Temoporfin-mediated photodynamic therapy in patients with advanced, incurable head and neck cancer: A multicenter study. *Head & neck* **2010**, *32* (12), 1597−1604.
(32) Nathan, T. R.; Whitelaw, D. E.; Chang, S. C.; Lees, W. R.; Ripley, P. M.; Payne, H.; Jones, L.; Parkinson, M. C.; Emberton, M.; Gillams, A. R.; et al. Photodynamic therapy for prostate cancer recurrence after radiotherapy: a phase I study. *Journal of urology* **2002**, *168* (4), 1427−1432.
(33) Trachtenberg, J.; Bogaards, A.; Weersink, R. A.; Haider, M. A.; Evans, A.; McCluskey, S. A.; Scherz, A.; Gertner, M. R.; Yue, C.; Appu, S.; et al. Vascular targeted photodynamic therapy with palladium-bacteriopheophorbide photosensitizer for recurrent prostate cancer following definitive radiation therapy: assessment of safety and treatment response. *Journal of urology* **2007**, *178* (5), 1974−1979.
(34) Muller, P. J.; Wilson, B. C. Photodynamic therapy of malignant brain tumours. *Lasers in Medical Science* **1990**, *5* (2), 245−252.
(35) Umegaki, N.; Moritsugu, R.; Katoh, S.; Harada, K.; Nakano, H.; Tamai, K.; Hanada, K.; Tanaka, M. Photodynamic therapy may be useful in debulking cutaneous lymphoma prior to radiotherapy. *Clinical and Experimental Dermatology: Clinical dermatology* **2004**, *29* (1), 42−45.
(36) Lam, S.; Kostashuk, E. C.; Coy, E. P.; Laukkanen, E.; LeRiche, J. C.; Mueller, H. A.; Szasz, I. J. A randomized comparative study of the safety and efficacy of photodynamic therapy using Photofrin II combined with palliative radiotherapy versus palliative radiotherapy alone in patients with inoperable obstructive non-small cell bronchogenic carcinoma. *Photochemistry and photobiology* **1987**, *46* (5), 893−897.
(37) Imamura, S.; Kusunoki, Y.; Takifuji, N.; Kudo, S.; Matsui, K.; Masuda, N.; Takada, M.; Negoro, S.; Ryu, S.; Fukuoka, M. Photodynamic therapy and/or external beam radiation therapy for roentgenologically occult lung cancer. *Cancer* **1994**, *73* (6), 1608−1614.
(38) Calzavara, F.; Tomio, L.; Corti, L.; Zorat, P. L.; Barone, I.; Peracchia, A.; Norberto, L.; D'Arcais, R. F.; Berti, F. Oesophageal cancer treated by photodynamic therapy alone or followed by

https://doi.org/10.1021/acsbiomaterials.2c00287
ACS Biomater. Sci. Eng. XXXX, XXX, XXX−XXX

radiation therapy. *Journal of Photochemistry and Photobiology B: Biology* **1990**, *6* (1−2), 167−174.
(39) Weinberg, B. D.; Allison, R. R.; Sibata, C.; Parent, T.; Downie, G. Results of combined photodynamic therapy (PDT) and high dose rate brachytherapy (HDR) in treatment of obstructive endobronchial non-small cell lung cancer (NSCLC). *Photodiagnosis and photodynamic therapy* **2010**, *7* (1), 50−58.
(40) Nakano, A.; Watanabe, D.; Akita, Y.; Kawamura, T.; Tamada, Y.; Matsumoto, Y. Treatment efficiency of combining photodynamic therapy and ionizing radiation for Bowen's disease. *Journal of the European Academy of Dermatology and Venereology* **2011**, *25* (4), 475−478.
(41) Yan, J.; Li, B.; Yang, P.; Lin, J.; Dai, Y. Progress in Light-Responsive Lanthanide Nanoparticles toward Deep Tumor Theranostics. *Adv. Funct. Mater.* **2021**, *31* (42), 2104325.
(42) Kamkaew, A.; Chen, F.; Zhan, Y.; Majewski, R. L.; Cai, W. Scintillating Nanoparticles as Energy Mediators for Enhanced Photodynamic Therapy. *ACS Nano* **2016**, *10* (4), 3918−3935.
(43) Chong, L. M.; Tng, D. J. H.; Tan, L. L. Y.; Chua, M. L. K.; Zhang, Y. Recent advances in radiation therapy and photodynamic therapy. *Applied Physics Reviews* **2021**, *8* (4), 041322.
(44) Cline, B.; Delahunty, I.; Xie, J. Nanoparticles to mediate X-ray-induced photodynamic therapy and Cherenkov radiation photodynamic therapy. *Wiley Interdiscip Rev Nanomed Nanobiotechnol* . **2019**, *11* (2), No. e1541.
(45) Chen, W.; Zhang, J. Using Nanoparticles to Enable Simultaneous Radiation and Photodynamic Therapies for Cancer Treatment. *J. Nanosci. Nanotechnol.* **2006**, *6* (4), 1159−1166.
(46) Chen, H.; Sun, X.; Wang, G. D.; Nagata, K.; Hao, Z.; Wang, A.; Li, Z.; Xie, J.; Shen, B. LiGa 5 O 8: Cr-based theranostic nanoparticles for imaging-guided X-ray induced photodynamic therapy of deep-seated tumors. *Materials horizons* **2017**, *4* (6), 1092−1101.
(47) Ahmad, F.; Wang, X.; Jiang, Z.; Yu, X.; Liu, X.; Mao, R.; Chen, X.; Li, W. Codoping enhanced radioluminescence of nanoscintillators for x-ray-activated synergistic cancer therapy and prognosis using metabolomics. *ACS Nano* **2019**, *13* (9), 10419−10433.
(48) Jiang, Z.; He, L.; Yu, X.; Yang, Z.; Wu, W.; Wang, X.; Mao, R.; Cui, D.; Chen, X.; Li, W. Antiangiogenesis Combined with Inhibition of the Hypoxia Pathway Facilitates Low-Dose, X-ray-Induced Photodynamic Therapy. *ACS Nano* **2021**, *15* (7), 11112−11125.
(49) Clement, S.; Chen, W.; Anwer, A. G.; Goldys, E. M. Verteprofin conjugated to gold nanoparticles for fluorescent cellular bioimaging and X-ray mediated photodynamic therapy. *Microchimica Acta* **2017**, *184* (6), 1765−1771.
(50) Deng, W.; McKelvey, K. J.; Guller, A.; Fayzullin, A.; Campbell, J. M.; Clement, S.; Habibalahi, A.; Wargocka, Z.; Liang, L.; Shen, C.; et al. Application of Mitochondrially Targeted Nanoconstructs to Neoadjuvant X-ray-Induced Photodynamic Therapy for Rectal Cancer. *ACS Central Science* **2020**, *6* (5), 715−726.
(51) Sun, W.; Luo, L.; Feng, Y.; Cai, Y.; Zhuang, Y.; Xie, R.-J.; Chen, X.; Chen, H. Aggregation-Induced Emission Gold Clustoluminogens for Enhanced Low-Dose X-ray-Induced Photodynamic Therapy. *Angew. Chem., Int. Ed.* **2020**, *59* (25), 9914−9921.
(52) Sherck, N. J.; Won, Y.-Y. Technical Note: A simulation study on the feasibility of radiotherapy dose enhancement with calcium tungstate and hafnium oxide nano- and microparticles. *Medical Physics* **2017**, *44* (12), 6583−6588.
(53) Jo, S. D.; Lee, J.; Joo, M. K.; Pizzuti, V. J.; Sherck, N. J.; Choi, S.; Lee, B. S.; Yeom, S. H.; Kim, S. Y.; Kim, S. H.; Kwon, I. C.; Won, Y. Y. PEG-PLA-Coated and Uncoated Radio-Luminescent CaWO4-Micro- and Nanoparticles for Concomitant Radiation and UV-A/Radio-Enhancement Cancer Treatments. *Acs Biomaterials Science & Engineering* **2018**, *4* (4), 1445−1462.
(54) Lee, J.; Rancilio, N. J.; Poulson, J. M.; Won, Y.-Y. Block Copolymer-Encapsulated CaWO4 Nanoparticles: Synthesis, Formulation, and Characterization. *ACS Appl. Mater. Interfaces* **2016**, *8* (13), 8608−8619.
(55) Pizzuti, V.; Viswanath, D.; Torregrosa-Allen, S. E.; Currie, M. P.; Elzey, B. D.; Won, Y.-Y. Bilirubin-Coated Radio-Luminescent Particles for Radiation-Induced Photodynamic Therapy. *ACS Applied Bio Materials* **2020**, *3*, 4858−4872.
(56) Pizzuti, V. J.; Misra, R.; Lee, J.; Torregrosa-Allen, S. E.; Currie, M. P.; Clark, S. R.; Patel, A. P.; Schorr, C. R.; Jones-Hall, Y.; Childress, M. O.; Plantenga, J. M.; Rancilio, N. J.; Elzey, B. D.; Won, Y.-Y. Folic Acid-Conjugated Radioluminescent Calcium Tungstate Nanoparticles as Radio-Sensitizers for Cancer Radiotherapy. *ACS Biomaterials Science & Engineering* **2019**, *5* (9), 4776−4789.
(57) Lismont, M.; Dreesen, L.; Wuttke, S. Metal-organic framework nanoparticles in photodynamic therapy: current status and perspectives. *Adv. Funct. Mater.* **2017**, *27* (14), 1606314.
(58) Liu, J.; Yang, Y.; Zhu, W.; Yi, X.; Dong, Z.; Xu, X.; Chen, M.; Yang, K.; Lu, G.; Jiang, L.; et al. Nanoscale metal- organic frameworks for combined photodynamic & radiation therapy in cancer treatment. *Biomaterials* **2016**, *97*, 1−9.
(59) Lan, G.; Ni, K.; Xu, R.; Lu, K.; Lin, Z.; Chan, C.; Lin, W. Nanoscale metal-organic layers for deeply penetrating X-ray-induced photodynamic therapy. *Angew. Chem.* **2017**, *129* (40), 12270−12274.
(60) Phase I Study of RiMO-301 With Radiation in Advanced Tumors. https://clinicaltrials.gov/ct2/show/NCT03444714 (accessed on March 9, 2022).
(61) Ma, L.; Chen, W.; Schatte, G.; Wang, W.; Joly, A. G.; Huang, Y.; Sammynaiken, R.; Hossu, M. A new Cu-cysteamine complex: structure and optical properties. *Journal of Materials Chemistry C* **2014**, *2* (21), 4239−4246.
(62) Liu, Z.; Xiong, L.; Ouyang, G.; Ma, L.; Sahi, S.; Wang, K.; Lin, L.; Huang, H.; Miao, X.; Chen, W.; Wen, Y. Investigation of Copper Cysteamine Nanoparticles as a New Type of Radiosensitiers for Colorectal Carcinoma Treatment. *Sci. Rep.* **2017**, *7* (1), 9290.
(63) Shrestha, S.; Wu, J.; Sah, B.; Vanasse, A.; Cooper, L. N.; Ma, L.; Li, G.; Zheng, H.; Chen, W.; Antosh, M. P. X-ray induced photodynamic therapy with copper-cysteamine nanoparticles in mice tumors. *Proc. Natl. Acad. Sci. U. S. A.* **2019**, *116* (34), 16823−16828.
(64) Wang, H.; Lv, B.; Tang, Z.; Zhang, M.; Ge, W.; Liu, Y.; He, X.; Zhao, K.; Zheng, X.; He, M.; et al. Scintillator-based nanohybrids with sacrificial electron prodrug for enhanced x-ray-induced photodynamic therapy. *Nano Lett.* **2018**, *18* (9), 5768−5774.
(65) Daouk, J.; Dhaini, B.; Petit, J.; Frochot, C.; Barberi-Heyob, M.; Schohn, H. Can Cerenkov Light Really Induce an Effective Photodynamic Therapy? *Radiation* **2021**, *1* (1), 5−17.
(66) Kotagiri, N.; Sudlow, G. P.; Akers, W. J.; Achilefu, S. Breaking the depth dependency of phototherapy with Cerenkov radiation and low-radiance-responsive nanophotosensitizers. *Nat. Nanotechnol.* **2015**, *10* (4), 370−379.
(67) Duan, D.; Liu, H.; Xu, Y.; Han, Y.; Xu, M.; Zhang, Z.; Liu, Z. Activating TiO_2 Nanoparticles: Gallium-68 Serves as a High-Yield Photon Emitter for Cerenkov-Induced Photodynamic Therapy. *ACS Appl. Mater. Interfaces* **2018**, *10* (6), 5278−5286.
(68) Ni, D.; Ferreira, C. A.; Barnhart, T. E.; Quach, V.; Yu, B.; Jiang, D.; Wei, W.; Liu, H.; Engle, J. W.; Hu, P.; Cai, W. Magnetic Targeting of Nanotheranostics Enhances Cerenkov Radiation-Induced Photodynamic Therapy. *J. Am. Chem. Soc.* **2018**, *140* (44), 14971−14979.
(69) Li, J.; Dai, S.; Qin, R.; Shi, C.; Ming, J.; Zeng, X.; Wen, X.; Zhuang, R.; Chen, X.; Guo, Z.; et al. Ligand Engineering of Titanium-Oxo Nanoclusters for Cerenkov Radiation-Reinforced Photo/Chemodynamic Tumor Therapy. *ACS Appl. Mater. Interfaces* **2021**, *13* (46), 54727−54738.
(70) Chen, Y.-A.; Li, J.-J.; Lin, S.-L.; Lu, C.-H.; Chiu, S.-J.; Jeng, F.-S.; Chang, C.-W.; Yang, B.-H.; Chang, M.-C.; Ke, C.-C.; Liu, R.-S. Effect of Cerenkov Radiation-Induced Photodynamic Therapy with 18F-FDG in an Intraperitoneal Xenograft Mouse Model of Ovarian Cancer. *International Journal of Molecular Sciences* **2021**, *22* (9), 4934.
(71) Qian, R.; Wang, K.; Guo, Y.; Li, H.; Zhu, Z.; Huang, X.; Gong, C.; Gao, Y.; Guo, R.; Yang, B.; Wang, C.; Jiang, D.; Lan, X.; An, R.; Gao, Z. Minimizing adverse effects of Cerenkov radiation induced photodynamic therapy with transformable photosensitizer-loaded nanovesicles. *J. Nanobiotechnol.* **2022**, *20* (1), 1−15.

https://doi.org/10.1021/acsbiomaterials.2c00287
ACS Biomater. Sci. Eng. XXXX, XXX, XXX−XXX

(72) Hall, E. J.; Giaccia, A. J. *Radiobiology for the Radiologist*; Lippincottt Williams & Wilkins: Philadelphia, PA, 2006; Vol. *6*.
(73) Sun, W.; Zhou, Z.; Pratx, G.; Chen, X.; Chen, H. Nanoscintillator-Mediated X-Ray Induced Photodynamic Therapy for Deep-Seated Tumors: From Concept to Biomedical Applications. *Theranostics* **2020**, *10* (3), 1296−1318.
(74) Rim, K. T.; Koo, K. H.; Park, J. S. Toxicological evaluations of rare earths and their health impacts to workers: a literature review. *Safety and health at work* **2013**, *4* (1), 12−26.
(75) Ersoy, H.; Rybicki, F. J. Biochemical safety profiles of gadolinium-based extracellular contrast agents and nephrogenic systemic fibrosis. *Journal of Magnetic Resonance Imaging: An Official Journal of the International Society for Magnetic Resonance in Medicine* **2007**, *26* (5), 1190−1197.

https://doi.org/10.1021/acsbiomaterials.2c00287
ACS Biomater. Sci. Eng. XXXX, XXX, XXX−XXX